Tectonophysics 692 (2016) 120–130

Contents lists available at ScienceDirect

Tectonophysics

journal homepage: www.elsevier.com/locate/tecto

Distribution of stress state in the Nankai subduction zone, southwest Japan and a comparison with Japan Trench

Weiren Lin [a,b,*], Timothy B. Byrne [c], Masataka Kinoshita [d,e], Lisa C. McNeill [f], Chandong Chang [g], Jonathan C. Lewis [h], Yuzuru Yamamoto [i], Demian M. Saffer [j], J. Casey Moore [k], Hung-Yu Wu [e], Takeshi Tsuji [l], Yasuhiro Yamada [e], Marianne Conin [m], Saneatsu Saito [e], Takatoshi Ito [n], Harold J. Tobin [o], Gaku Kimura [p], Kyuichi Kanagawa [q], Juichiro Ashi [r], Michael B. Underwood [s], Toshiya Kanamatsu [t]

[a] Graduate School of Engineering, Kyoto University, Kyoto, Japan
[b] Kochi Institute for Core Sample research, Japan Agency for Marine-Earth Science and Technology, Nankoku, Japan
[c] Center for Integrative Geosciences, University of Connecticut, Storrs, CT, USA
[d] Earthquake Research Institute, University of Tokyo, Tokyo, Japan
[e] Research and Development Center for Ocean Drilling Science, Japan Agency for Marine-Earth Science and Technology, Yokohama, Japan
[f] Southampton Oceanography Centre, University of Southampton, Southampton, UK
[g] Department of Geology, Chungnam National University, Daejeon, Republic of Korea
[h] Department of Geoscience, Indiana University of Pennsylvania, Indiana, PA, USA
[i] Department of Mathematical Science and Advanced Technology, Japan Agency for Marine and Earth Science and Technology, Yokohama, Japan
[j] Department of Geosciences and Center for Geofluids, Geomechanics, and Geohazards, The Pennsylvania State University, University Park, PA, USA
[k] Earth and Planetary Sciences Department, University of California, Santa Cruz, CA, USA
[l] International Institute for Carbon-Neutral Energy Research, Kyushu University, Fukuoka, Japan
[m] University of Lorraine, ENSMN, Nancy, France
[n] Institute of Fluid Science, Tohoku University, Sendai, Japan
[o] Department of Geoscience, Univ. WI-Madison, Madison, WI, USA
[p] Department of Earth and Planetary Science, The University of Tokyo, Tokyo, Japan
[q] Department of Earth Sciences, Chiba University, Chiba, Japan
[r] Atmosphere and Ocean Research Institute, The University of Tokyo, Tokyo, Japan
[s] Department of Geological Science, University of MO, Columbia, MO, USA
[t] Research and Development Center for Earthquake and Tsunami, Japan Agency for Marine-Earth Science and Technology, Yokosuka, Japan

ARTICLE INFO

Article history:
Received 10 September 2014
Received in revised form 2 April 2015
Accepted 20 May 2015
Available online 30 May 2015

Keywords:
Stress state
Nankai subduction zone
Japan Trench
Ocean drilling

ABSTRACT

To better understand the distribution of three dimensional stress states in the Nankai subduction zone, southwest Japan, we review various stress-related investigations carried out in the first and second stage expeditions of the Nankai Trough Seismogenic Zone Experiment (NanTroSEIZE) by the Integrated Ocean Drilling Program (IODP) and compile the stress data. Overall, the maximum principal stress σ_1 in the shallower levels (<~1 km) is vertical from near the center of forearc basin to near the trench and; the maximum horizontal stress S_{Hmax} (interpreted to be the intermediate principal stress σ_2) is generally parallel to the plate convergence vector. The exception to this generalization occurs along the shelf edge of the Nankai margin where S_{Hmax} is along strike rather than parallel to the plate convergence vector. Reorientation of the principal stresses at deeper levels (e.g., >~1 km below seafloor or in underlying accretionary prism) with σ_1 becoming horizontal is also suggested at all deeper drilling sites. We also make a comparison of the stress state in the hanging wall of the frontal plate-interface between Site C0006 in the Nankai and Site C0019 in the Japan Trench subduction zone drilled after the 2011 Mw 9.0 Tohoku-Oki earthquake. In the Japan Trench, a comparison between stress state before and after the 2011 mega-earthquake shows that the stress changed from compression before the earthquake to extension after the earthquake. As a result of the comparison between the Nankai Trough and Japan Trench, a similar current stress state with trench parallel extension was recognized at both C0006 and C0019 sites. Hypothetically, this may indicate that in Nankai Trough it is still in an early stage of the interseismic cycle of a great earthquake which occurs on the décollement and propagates to the toe (around site C0006).

1. Introduction

Stress and earthquakes are known to be interrelated: stress triggers earthquakes and earthquakes alter the shear and normal stresses on surrounding faults (Hardebeck, 2004; Lin et al., 2007; Ma et al., 2005;

* Corresponding author at: Graduate School of Engineering, Kyoto University, C1-1-109 C-cluster, Kyoto Daigaku Katsura, Nishikyo-ku, Kyoto 615-8540, Japan.
Fax: +81 75 383 3203.
E-mail address: lin@kumst.kyoto-u.ac.jp (W. Lin).

http://dx.doi.org/10.1016/j.tecto.2015.05.008
0040-1951/

Seeber and Armbruster, 2000; Stein, 1999). On the other hand, the stresses both on the fault and in the formation gradually build up in the interseismic period (Kanamori and Brodsky, 2001). The Nankai Trough Seismogenic Zone Experiment (NanTroSEIZE), a comprehensive scientific drilling project conducted by the Integrated Ocean Drilling Program (IODP) in the Nankai subduction zone, southwest Japan, is designed to investigate the mechanics of the subduction megathrust through drilling and a wide range of allied studies (Tobin and Kinoshita, 2006; Tobin et al., 2009a). In this area, Mw 8.0 class great earthquakes repeat at intervals of 100–200 years as a result of the convergence of the Philippine Sea and Eurasian plates (Ando, 1975; Fig. 1). The last two great earthquakes in the Nankai subduction zone occurred in 1944 (Tonankai, M 8.0–8.3) and 1946 (Nankai, M 8.1–8.4), generating tsunamis and causing significant damage in southwest Japan (Kanamori 1972). The NanTroSEIZE project sampled and continues to monitor the characteristics of the seismogenic zone during the interseismic interval. In contrast, IODP expedition 343 to the Japan Trench (also referred to as the Japan Trench Fast Drilling Project or JFAST), was conducted just after a great earthquake, about 13 months after the 2011 Mw 9.0 Tohoku-Oki, Japan earthquake (Mori et al., 2012; Chester et al., 2012; Fig. 1).

Establishing the in situ stress state along active subduction zones is critical for understanding the accumulation and release of most of Earth's seismic energy (Lallemand and Funiciello, 2009). Determination of in situ stress is one of the most important scientific objectives of both NanTroSEIZE and JFAST, and also one of the major goals of the IODP as the seismogenic parts of plate margins are often only accessible through drilling. First, we review various stress-related investigations carried out in association with NanTroSEIZE stages 1 and 2. We then compare the present-day stress states in the frontal part of the plate-interface at the Nankai and Japan Trench subduction zones and propose hypotheses on the temporal and spatial evolution of stresses in the frontal plate-interface in Nankai, SW Japan.

2. Stress estimates and direct measurements from stages 1 and 2 of the NanTroSEIZE drilling project

The multi-stage scientific drilling project NanTroSEIZE, conducted by the drilling vessel D/V *Chikyu*, began in 2007 with IODP expedition 314 and is continuing with planned deep riser drilling in the coming years (Hirose et al., 2013; Kinoshita et al., 2008). To date more than 10 drilling sites have been drilled along the NanTroSEIZE transect with at least one vertical borehole(s) at each site. This transect is approximately orthogonal to the Nankai Trough axis (plate boundary) (Figs. 2, 3 and 4a and Table 1).

In the first stage of NanTroSEIZE (2007–2008), borehole wall images obtained by logging while drilling (LWD) technology yielded regional patterns of stress orientations and magnitudes through observations of drilling-induced compressive failures (borehole breakouts) and tensile fractures (DITFs) (e.g., Chang et al, 2010; Lee et al., 2013; Lin et al., 2010a; Moore et al., 2011; Tobin et al., 2009b). This stage involved five drilling sites in three structural settings in which LWD was performed: the frontal thrust at the toe of the accretionary prism, Site C0006; the megasplay hanging wall and footwall, Sites C0010, C0004 and C0001, and the seaward edge of the Kumano forearc basin, Site C0002 (Figs. 2, 3 and 4a). These regional studies were followed by more detailed core-based analyses and geophysical studies, including interpretation of high-resolution seismic reflection data and S-wave splitting that provided a three-dimensional understanding of the stress field and the evolution of stresses through time (Byrne et al., 2009; Conin et al., 2014; Kimura et al., 2011; Lewis et al., 2013; Moore et al., 2013; Sacks

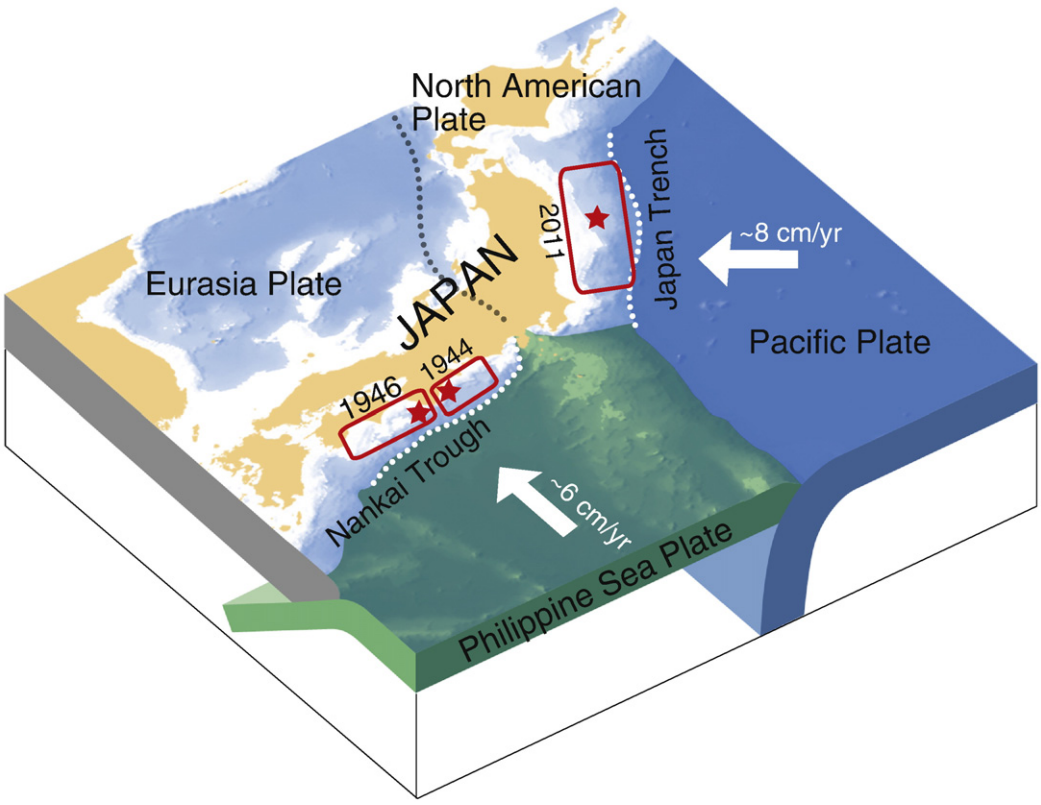

Fig. 1. Nankai and Japan Trench subduction zones and plates around Japan islands. Red stars and numbers show the epicenters of the earthquakes and its occurrence year; the red frames are the area of rupture zones during the earthquakes. White arrows and numbers show directions and rates of plate motion, respectively (Apel et al., 2006; Loveless and Meade, 2010; Ozawa et al., 2011; Sella et al., 2002).

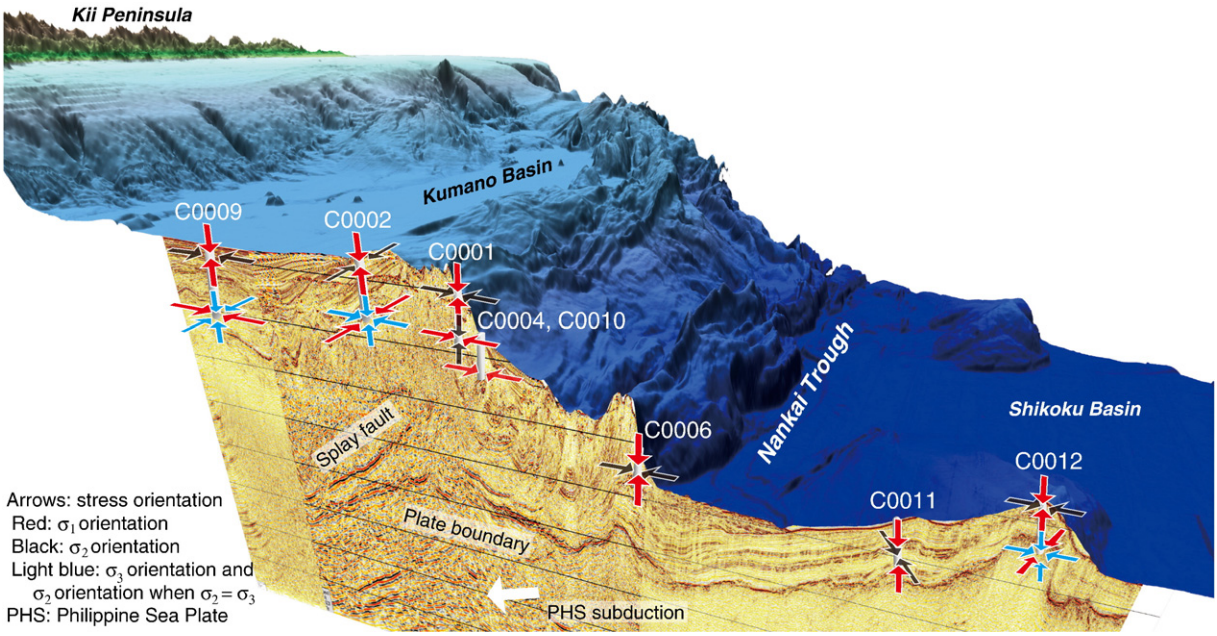

Fig. 2. Distributions of semi three-dimensional stress state in NanTroSEIZE transect. Codes (e.g. C0009) are the number of drilling sites. Red, black and light blue arrows are the orientations of the maximum, intermediate and minimum principal stresses, respectively. Two pair arrows in the same light blue color in the deeper part of C0009, C0002 and C0012 mean that the intermediate and minimum principal stresses are nearly equal each other, or the intermediate and minimum principal stresses are highly variable.

et al., 2013; Tsuji et al., 2011a). Taken together, these results show that at all sites except C0004 and C0010, the maximum principal stress σ_1 is vertical at shallow levels and that the orientation of the intermediate principal stress σ_2 changes from trench perpendicular at C0006 and C0001 to trench parallel at C0002. At sites C0004 and C0010 σ_1 is interpreted possibly to be horizontal and approximately parallel to the plate convergent direction.

In the second stage of NanTroSEIZE (2009–2010), D/V *Chikyu* carried out the first riser drilling in IODP history at Site C0009 of Expedition 319. This expedition targeted the hanging wall above the high slip region of the 1944 Tonankai earthquake (Saffer et al., 2009). The borehole penetrated the Kumano forearc basin sediments and the underlying accretionary prism; and was the deepest drilling (~1.6 km) during the first and second stages of NanTroSEIZE. In a depth range from approximately 700 mbsf (meters below seafloor) to the target depth of 1600 mbsf, wireline logging included a borehole caliper and a fullbore formation microimager (FMI) that provided resistivity images. From the borehole images and caliper data, borehole breakouts and DITFs were identified and the horizontal stress orientations were obtained (Lin et al., 2010a; Saffer et al., 2009; Wu et al., 2012). Due to limited azimuthal coverage (~50%) of the wellbore walls by FMI, the width of breakouts was not well constrained, and therefore no reliable information about stress magnitudes could be extracted from the wellbore failures.

The first hydraulic fracturing experiments in the scientific ocean drilling history also were carried out using two techniques at Site C0009. The first, an "extended leak-off test", was conducted as part of drilling operations and provided a measurement of minimum principal stress magnitude at ~708 mbsf (Lin et al., 2008; Saffer et al., 2013). The second technique, a "two dual-packer hydraulic fracture test" was conducted using Modular Dynamic Tester (MDT) tool (Haimson and Cornet, 2003; Ito et al., 2013; Saffer et al., 2013), and yielded two additional measurements of in situ minimum principal stress magnitude: one at ~877 mbsf and a less reliable determination at ~1534 mbsf. Drill core samples were also recovered in a ~80 m depth interval in mudstones interpreted as either the uppermost accretionary prism or a paleo-slope basin. Anelastic strain recovery (ASR) measurements on core samples were used to determine the three-dimensional stress

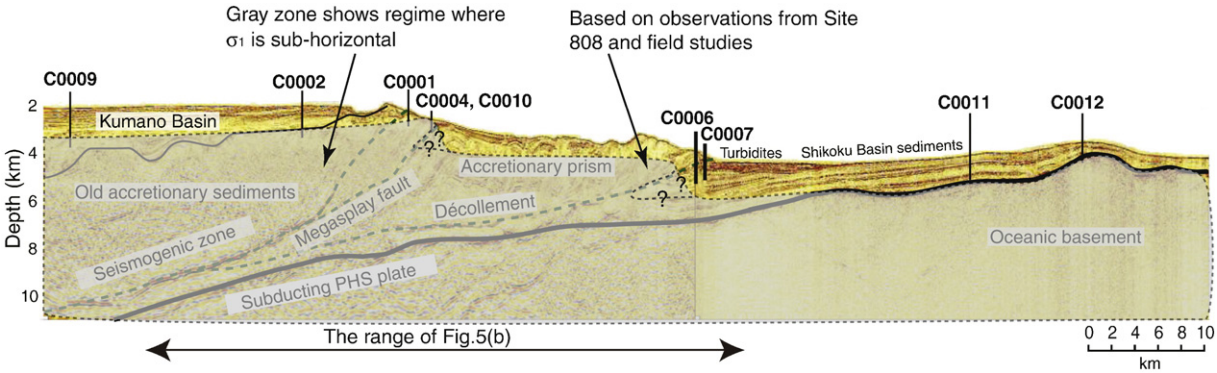

Fig. 3. Seismic reflection section of NanTroSEIZE transect (modified from Saito et al., 2009). Depths denote the depth below sea level. The gray overlay shows the predicted area of horizontal σ_1 (the maximum principal stress). Around megasplay site C0004 and the frontal thrust site C0006, two patterns of σ_1 distribution are considered to be possible. The first one is a gradual change; but the other shows a drastic change around the decollement and the megasplay suggested from the observations at ODP Site 808 and Alaska (Byrne & Fisher, 1990 and Lallemant et al., 1993).

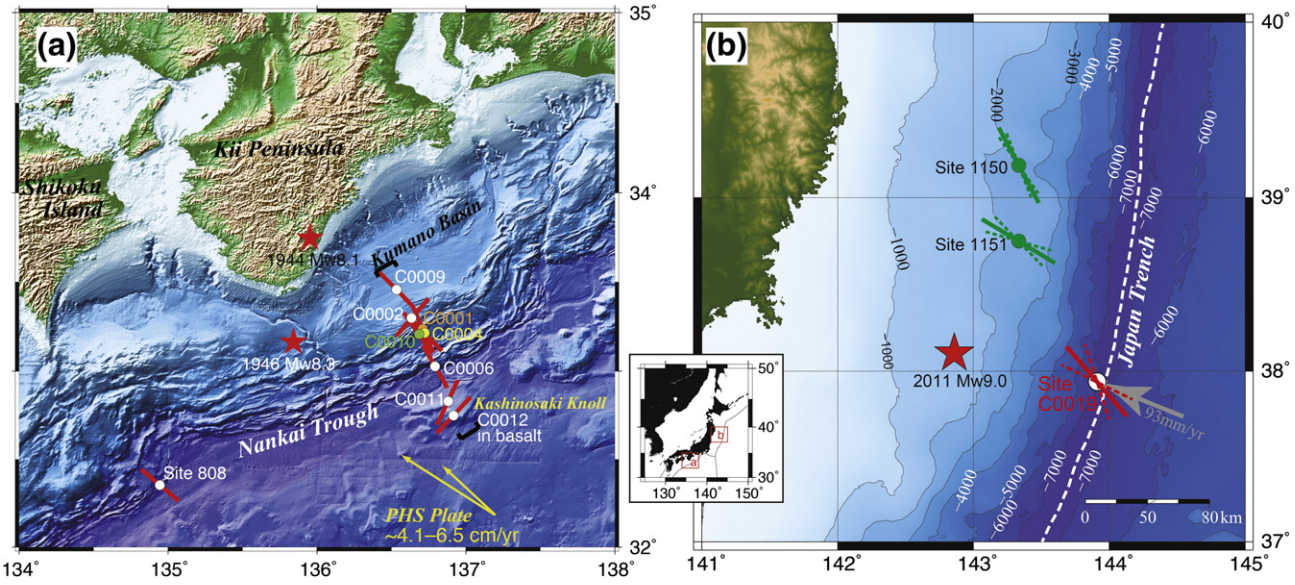

Fig. 4. The maximum horizontal stress (S_{Hmax}) orientations in SW and NE Japan subduction zones. Red bars at the drilling sites show the representative S_{Hmax} orientations in the sites. Two rad rectangles in inset show locations of figures (a) and (b), respectively. (a) Stress orientations at Site C0009 compiled from Lin et al. (2010a) and Wu et al. (2012); C0002, C0001, C0004 and C0006 from Chang et al. (2010), C0011 from Expedition 322 Scientists (2010), C0012 from Yamamoto et al. (2013), and at ODP Site 808 from McNeill et al. (2004) and Ienaga et al. (2006). Yellow arrows show the far-field convergence vectors between the Philippine Sea plate and Japan (Heki and Miyazaki, 2001; Miyazaki and Heki, 2001). (b) Location of JFAST Site C0019 and S_{Hmax} orientation in the deep part of the borehole (Lin et al., 2013). Red solid and dashed lines show the mean S_{Hmax} orientation and one standard deviation (SD), respectively, determined in 2012 after the 2011 Tohoku earthquake. Green circles and lines show ODP sites drilled in 1999 and their S_{Hmax} orientations prior to the 2011 earthquake (Lin et al., 2011). The gray arrow shows relative plate motion around Site C0019 (Argus et al., 2011). The white numbers and the contour lines show water depths.

orientations by the same method as Byrne et al. (2009) (Lin et al., 2010b). In addition, results of a "walkaround" vertical seismic profiling (VSP) experiment recorded at Site C0009 and conducted by D/V *Chikyu* and R/V *Kairei* showed a clear anisotropy in P wave velocity and amplitude, and documented S wave splitting. These data have also been interpreted as indicators of horizontal stress orientations (Tsuji et al., 2011b).

During IODP expeditions 322 in stage 2, two reference sites were drilled on the incoming Philippine Sea Plate: Site C0012, located ~31 km seaward of the trench on basement high to sample a condensed sedimentary section, and Site C0011, ~22 km seaward of the trench designed to sample the section at a basement low. LWD resistivity images documented borehole breakouts and provide an indication of horizontal principal stress orientations at Site C0011 (Expedition 322 Scientists, 2010; Wu et al., 2013). Site C0012 was not drilled with LWD; however, ASR measurements on core samples yielded constraints on stress states in both the oceanic crust (basalt) and the sedimentary cover (Yamamoto et al., 2013).

3. Results of stage 1 drilling, Nankai subduction zone, SW Japan

3.1. C0001

Borehole breakouts, tensile fractures and core-scale faults are present in the upper half of the boreholes at Site C0001 and provide constraints on the orientation, ratios and magnitudes of the principal stresses (Expedition 314 Scientists, 2009a). The maximum horizontal stress S_{Hmax} orientation determined from borehole breakouts and tensile fractures consistently trend ~335° throughout the hole, although Chang et al. (2010) proposed that the stress regime changes with depth, likely

Table 1
Specifications of the stress measurement related boreholes in NanTroSEIZE and JFAST drilling sites. For example, C0002 denotes the drilling site; whereas C0002A is the name of the borehole "A" located at Site C0002. Usually, multi boreholes were drilled for different operations within a narrow area (e.g. a few tens meters) in a site in IODP.

Holes (stress related operations)	Location		Water depth m	Total depth mbsf	Source of data
	Latitude	Longitude			
C0009A (WL&C[a])	33°27.47′N	136°32.15′E	2054	1604	Exp 319 Summary
C0002A (LWD[b])	33°18.02′N	136°38.18′E	1936	1402	Exp 314 Summary
C0002B (Coring)	33°17.99′N	136°38.20′E	1938	1057	Exp 315 Summary
C0001D (LWD)	33°14.33′N	136°42.70′E	2198	976	Exp 314 Summary
C0001E (Coring)	33°14.34′N	136°42.69′E	2198	118	Exp 315 Summary
C0001F (Coring)	33°14.34′N	136°42.71′E	2197	249	Exp 315 Summary
C0004B (LWD)	33°13.23′N	136°43.35′E	2637	400	Exp 314 Summary
C0010A (LWD)	33°12.60′N	136°41.12′E	2524	555	Exp 319 Summary
C0006B (LWD)	33°01.64′N	136°47.64′E	3872	886	Exp 314 Summary
C0006E (Coring)	33°01.64′N	136°47.63′E	3876	409	Exp 316 Summary
C0011A (LWD)	32°49.73′N	136°52.89′E	4049	952	Exp 319 Summary
C0012A (Coring)	32°44.89′N	136°55.02′E	3511	576	Exp 322 Summary
C0019B (LWD)	37°56.34′N	143°54.81′E	6890	851	Exp 343 Summary

[a] WL&C: Wireline logging and coring.
[b] LWD: Logging While Drilling.

due to increasing S_{Hmax} (Fig. 2). At shallow levels (<~500 mbsf) S_{Hmax} is interpreted to be σ_2 and smaller in magnitude than the vertical stress, reflecting a normal faulting regime. Consolidation and triaxial compression tests of slope sediments in the uppermost ~200 mbsf also suggest horizontal effective stresses are ~41% of the vertical effective stress consistent with a normal faulting regime (Song et al., 2011). Stress inversion of core-scale faults from C0001 provides a measure of the three-dimensional stress state at relatively shallow levels and also shows normal faulting with extension parallel to the margin (Lewis et al., 2013). These results are consistent with faulting patterns observed in seismic reflection data as well as with the borehole breakout data that show σ_2 subparallel to the plate convergence vector. Lewis et al. (2013) also recognized an older suite of faults that, when inverted for stress orientations, show σ_1 trending northwest, parallel to the plate convergence vector. Chang et al. (2010) interpret S_{Hmax} at deeper levels (> ~ 500 mbsf) to be σ_1, reflecting a change with depth from normal faulting to strike-slip, or possibly thrusting. Unfortunately, sediment cores were not retrieved from deeper levels where the principal stresses appear to permutate.

3.2. C0002

Site C0002, which penetrated the Kumano forearc basin and the upper part of the underlying accretionary prism, also shows a consistent orientation of borehole breakouts with depth and a possible permutation of stresses with depth. S_{Hmax} determined from breakouts, however, trend northeast, approximately perpendicular to S_{Hmax} at C0001, which is only 10 km to the southeast (Figs. 2 and 3). Analysis of the breakouts, results from ASR experiments and inversion of core-scale faults show a normal faulting regime in the forearc sequence with the minimum principal stress σ_3 nearly parallel to the plate convergence vector and perpendicular to the shelf break. These results are consistent with numerous margin parallel normal faults observed in seismic reflection data (Gulick et al., 2010; Moore et al., 2013; Sacks et al., 2013). Many of the faults also cut the seafloor, suggesting that they are active or recently active, and the lack of growth data suggests that the transition to an extension dominated basin occurred less than ~1 Ma ago (Gulick et al, 2010). Sacks et al. (2013) and Moore et al. (2013) also show that there is a systematic change from any an early phase of generally trench-parallel extension that started before 0.44 Ma to trench-normal extension associated with faults that often cut the seafloor. These results are consistent with observations of core-scale fault populations that show a change from NE–SW extension to NW–SE extension (Expedition 315 Scientists, 2009). Chang et al. (2010) propose that the stress regime changes below the forearc sediments with S_{Hmax} becoming σ_1, suggesting a change from normal faulting to strike-slip or thrusting similar to the change proposed for Site C0001. The stress states at the two sites, however, are still fundamentally different as the borehole breakouts, and therefore S_{Hmax}, are perpendicular even at the deepest structural levels. In fact, the trend of S_{Hmax}, which is interpreted to be σ_1 in the deeper levels of C0002, suggests margin-parallel shortening rather than margin perpendicular shortening as interpreted for the deeper levels of C0001 (Fig. 2).

3.3. C0004

Site C0004 penetrated the megasplay fault, which appears to have slipped coseismically during the 1944 earthquake (Sakaguchi et al., 2011b) and borehole breakouts show consistent trends throughout the hole with S_{Hmax} trending northwest–southeast, approximately parallel to S_{Hmax} at C0001 (Expedition 314 Scientists, 2009b; Fig. 2). Site C0004 is only a few kms from C0001 and Byrne et al. (2009) assumed a relatively homogeneous stress field and proposed that S_{Hmax} at this site represented σ_2 rather than σ_1. More recent analyses of borehole breakouts, however, by Olcott and Saffer (2012) and Yamada and Shibanuma (2015) suggest that S_{Hmax} at this site possibly represents σ_1 consistent with a reverse or strike-slip faulting regime. They described that the magnitude of the vertical stress S_v may be smaller than that of S_{Hmax} but within the possible range of S_{hmin} (see Fig. 4 in Yamada and Shibanuma, 2015).

3.4. C0006

Site C0006 penetrated and sampled the hanging wall of the frontal thrust and borehole breakouts, anelastic strain and core-scale faults provide a more complete picture of the stress state than at C0004. Borehole breakouts occur throughout most of the hole although they appear much more weakly developed than at the other three sites. The breakouts trend 060° consistent with results from Sites C0001 and C004, indicating that S_{Hmax} trends about 330°, approximately parallel to the plate convergence vector (Expedition 314 Scientists, 2009c). ASR on a core sample from the hanging wall and inversion of the youngest suite of core-scale faults show a steeply plunging σ_1 with σ_3 trending northeast, indicating normal faulting and margin-parallel extension, similar to Site C0001 at shallow depths (Fig. 6b). Interpretations of the stress field around Site C0006 using a slip deficit model also indicate a normal faulting regime (Fig. 6a; Wu et al., 2013), and conjointly a significant erosion at the top of the slope sediments can be observed (Conin et al, 2011; Strasser et al, 2011). Anisotropy of magnetic susceptibility data (Byrne et al., 2009; Kitamura et al., 2010) and suites of core-scale structures that pre-date the normal faults show an earlier phase of margin-perpendicular shortening, which is also similar to the observations from Site C0001 (Lewis et al. 2013).

3.5. C0007

Site C0007, located less than a kilometer seaward of Site C0006 and a few hundred meters from the deformation front, was drilled after coring at Site C0006 failed to reach the frontal thrust (Fig. 3). Although the holes drilled at Site C0007 were not logged, so borehole images are not available, observations of cores indicate a deformation history similar to the history documented at Site C0006; that is, early northwest–southeast shortening followed by normal faulting. In addition, vitrinite reflectance measurements of samples from the frontal thrust show anomalously high temperatures, suggesting that the fault moved co-seismically (Sakaguchi et al., 2011a). Sites C0006 and C0007 together therefore may represent an analogous setting to Site C0019 in the Tohoku area which also sampled the front thrust after it slipped co-seismically.

4. Results from stage 2, Nankai subduction zone, SW Japan

4.1. C0009

At Site C0009, direct measurements of σ_3 via hydraulic fracturing tests and leak-off test (LOT) indicate that the stress regime changes from a normal faulting stress regime in the Kumano basin sediments to a possible strike-slip or thrusting stress regime in the underlying slope basin or accretionary wedge, to a depth of at least ~1600 mbsf similar to the change at Site C0001 (Fig. 2; Lin et al., 2010b; Ito et al., 2013; Saffer et al., 2013; Wu et al., 2013). Estimates of stress magnitude from the width of borehole breakouts at Site C0002 suggested a similar pattern, i.e. changing from a normal faulting stress regime in the basin sediments to a strike slip or thrust faulting regime in the underlying accretionary prism to the depth of ~1380 mbsf (the lower limit of breakout occurrence in borehole C0002A) (Byrne et al., 2009; Chang et al., 2010; Lee et al., 2013; Tobin et al., 2009a).

4.2. C0010

Site C0010 is located a few km along strike from Site C0004 and, similar to C0004, penetrated the hanging wall and footwall of the megasplay, one of primary drilling targets of the NanTroSEIZE. Shipboard analysis of the borehole breakouts showed a consistent pattern above

the megasplay with the maximum horizontal stress trending NW–SE (Expedition 319 Scientists, 2010). McNeill et al. (2010) noted that the megasplay corresponds to a seismic reflector with negative polar, suggesting a reduction in velocity and/or density in the footwall. They also recognized an abrupt change in orientation of the breakouts across the megasplay and proposed that the fault zone represented a sharp mechanical discontinuity. Although Olcott and Saffer (2012) proposed that σ_1 remained horizontal beneath in the footwall similar to the results from C0004, they also documented a shift to lower stress magnitudes in the footwall, based on the widths of borehole breakouts.

4.3. C0011 and C0012

At Site C0011, the orientation of S_{Hmax} was determined by borehole breakouts observed in a narrow depth interval (~600–650 mbsf, Expedition 322 Scientists, 2010) and is oblique to the plate convergence vector. Although estimates of stress magnitude are strongly dependent on assumed rock strength parameters, a normal faulting stress regime was suggested on the basis of wellbore breakout widths at ~610 mbsf (Wu et al., 2013).

At Site C0012, which is the most seaward input site and occurs on the crest of a prominent basement high (Kashinosaki Knoll), ASR results suggest a normal faulting regime in the sedimentary sequence, with S_{Hmax} oriented WNW–ESE (Yamamoto et al., 2013). In contrast, ASR analysis of a core sample of oceanic basement basalt shows a strike slip or a reverse faulting stress regime, with the maximum horizontal stress orientated northeast–southwest approximately parallel to the trough axis. The basement stress orientation could be the result of hinge extension during bending of the Philippine Sea plate, either in association with subduction or with the formation of an anticline during intraoceanic thrusting (Yamamoto et al., 2013).

5. Discussion: Nankai Margin

Although the drilling depths in stages 1 and 2 are relatively shallow (<~1.6 km at Site C0009), the results suggest important trends in both depth and map view. For example, observations at many of the sites suggest a change from a normal faulting regime at shallow structural levels to strike-slip or thrusting at deeper levels. These results suggest that gradients in topography may play an important role in defining the state of stress. Deeper drilling, like the programs completed as part of Expedition 348 which penetrated to ~3 kmbsf at Site C0002 and the future NanTroSEIZE expeditions planned to drill to >5 kmbsf in the same borehole will better define change in stress states with depth and provide a clearer understanding of how stress changes temporally and spatially in the prism.

The above review suggests two general patterns for the states of stress at relatively shallow levels: First, σ_1 appears to be vertical at all sites except in the hanging wall of the megasplay at Sites C0004 and C0010 where σ_1 is interpreted to be sub-horizontal and parallel to the plate convergence vector. Second, the maximum horizontal stresses S_{Hmax} appear to be parallel to the plate convergence vector except near the seaward edge of the Kumano Basin at Site C0002 where σ_3 is parallel to the plate convergence vector.

A possible explanation for the reorientation of σ_1 at C0004 and C0010 may be that the sediments being carried in the hanging wall are relatively strong and capable of supporting plate tectonic stresses. The occurrence of an extensional regime at higher structural levels where slope sediments are dominant (e.g., Site C0001) and the identification of a relatively weak footwall (McNeill et al, 2010; Olcott and Saffer, 2012) are consistent with this interpretation. We therefore propose that the hanging wall of the megasplay is relatively strong and supports a compressional stress state that is consistent with plate convergence. In contrast, the transmission of the stresses associated with plate convergence appears to be less effective in the slope sequence where σ_2 is observed to be parallel to the plate convergence vector and in the footwall where stress magnitudes decrease and possibly reorient. Drilling and sampling of core-scale faults across the décollement at Site 808 during the Ocean Drilling Program (ODP) Leg 131 along the Muroto transect also documented a reorientation of stresses (Lallemant et al., 1993). At this site σ_1 is sub-horizontal and NW-trending above the décollement, similar to the results from C0004 and C0010, and but sub-vertical below the décollement (Lallemant et al., 1993). One possibility is that the stresses below the megasplay have also been reoriented and σ_1 is vertical (Fig. 3) or they record a transition in stress states.

At C0002 the reorientation of σ_3 relative to the regional pattern may reflect gravitation collapse of the prism as the décollement weakens either continuously or during large earthquakes as suggested for the Tohoku region (Kimura et al., 2012; McKenzie and Jackson, 2012; Tsuji et al., 2013). A seismic reflection profile running NW–SE and including Site C0002 displays a clear sequence of trough-parallel normal faults in the basin sediments consistent with the maximum horizontal stress orientation data (e.g. Tobin et al., 2009a). Sacks et al. (2013) (and see also Moore et al., 2013) analyzed this regional-scale fault system in more detail and recognized two patterns of extension — an early phase of generally northeast–southwest, or margin-parallel, extension and a later phase of trench-perpendicular extension that is concentrated on the seaward edge of the basin. The fact that trench-perpendicular extension appears to be limited to the area of the shelf edge, which is both relatively far from the plate interface and at the topographic crest, is consistent with the hypothesis that gradients in topography (including effects of the "notch" proposed by Martin et al., 2010) are important in defining the state of stress along the margin. Theoretical studies as well as analog and numerical models also suggest that variations in the strength of the décollement below the wedge can lead to extension in the overlying accretionary wedge. For example, Haq and Davis (2008) show that for wedges with a ductile base, accretion can lead to over steepened topography and flow at lower structural levels, which drive trench-perpendicular extension (i.e., normal faulting) at higher structural levels. In fact, several authors have proposed that a regional low-velocity zone beneath the Nankai margin represents weak, and probably overpressured sediments (Bangs et al., 2009; Byrne et al. 2009; Kamei et al., 2012; Kitajima & Saffer, 2012; Park et al., 2010) that may act like the ductile lower crust in the analog models.

The above hypothesis for the pattern of regional-scale stresses, however, fails to consider the possible change in stresses associated with the earthquake cycle. For example, this region of the Nankai margin experienced a major earthquake and tsunami in 1944; and Sakaguchi et al. (2011a), based on maturation studies of vitrinite collected from fault zones sampled at Sites C0004 and C0007, proposed that megasplay and décollement slipped during the earthquake(s). Presumably, for some period before, and up to the beginning of the earthquake the state of stress in the hanging wall would have been compressional with σ_1 orientated sub-parallel to the plate convergence vector. The evidence from all of the sites along the Kumano transect where the principal stress orientations can be determined, however, shows a normal faulting regime, at least at shallow structural levels and excluding Sites C0004 and C0010 which sampled the hanging wall of the megasplay. These data also show that the rocks failed exclusively by normal faulting; that is, there is no evidence in the cores or seismic reflection data for alternating periods of extension and compression that could be interpreted as stress permutations associated with an earthquake cycle. For example, observation from Site C0002 and detailed studies of the deformation history in the Kumano Basin (Lewis et al., 2013 and Sacks et al., 2013, respectively) show an early phase of trench-parallel extension followed by a phase of trench-perpendicular extension. Neither data set shows stress permutations where the principal stresses switch multiple times, for example over several earthquake cycles. At least two explanations are possible, either: 1) all of the late stage normal faults formed after the last earthquake (e.g., after 1944) due to stress relaxation and stress permutations or 2) the stress states vary during the seismic cycle (e.g., σ_1 alternates between horizontal and vertical from one cycle to the next) (Conin et al.,

2012; Hashimoto et al., 2014; Kinoshita and Tobin, 2013; Sacks et al., 2013; Wang and Hu, 2006), but during an earthquake, failure is accommodated only or primarily by slip on major thrust faults and not on core-scale faults. After a major earthquake, the associated stress drop and relaxation leads to decrease in S_{Hmax}, such that the vertical stress S_v becomes σ_1, depending on the local stress field. Hsu et al. (2009) recently proposed an interpretation similar to the second alternative (#2 above) for stress permutations before and after the 1999 Chichi earthquake in Taiwan.

6. Stress states at the Japan Trench

6.1. IODP drilling Site C0019 and ODP Sites 1150 and 1151

The Japan Trench lies along the eastern edge of Japan and marks the boundary where the Pacific plate subducts beneath the Okhotsk plate (or North American plate) at ~8 cm/year (Loveless and Meade, 2010) (Fig. 1). The Tohoku-Oki earthquake (Mw 9.0) occurred on March 11, 2011 and was followed by a huge tsunami (Ide et al., 2011; Simons et al., 2011) that flooded many coastal regions of northeast Japan, taking over 18,000 lives. Planning for IODP Expedition 343 (informally called the "Japan Trench Fast Drilling Project" or JFAST) began soon after the earthquake with the primary goal of better understanding the stress and slip history along the fault. To this end, the goals of the expedition were to: 1) test the possibility that coseismic slip on a major fault generated frictional heat; 2) to investigate stress state on the fault and 3) retrieve samples from the proposed fault zone. To achieve these goals IODP expedition 343 conducted a rapid response drilling program about 13 months after the earthquake. The expedition successfully penetrated and sampled the frontal fault at a depth of ~820 mbsf at IODP Site C0019 where coseismic displacements were relatively large (~50 m) (Chester et al., 2012; Mori et al., 2012). Site C0019 is located ~93 km seaward from the epicenter of the mainshock of the Tohoku-Oki earthquake and ~6 km landward of the trench axis (Figs. 4b and 5).

In addition to the JFAST site, Sites 1150 and 1151, also located near the source area of the Tohoku-Oki earthquake, were drilled during ODP Leg 186 in 1999 prior to the earthquake (Lin et al., 2011) (Fig. 4b). Lin et al. (2011) integrated FMS images with caliper data to interpret the orientation of S_{Hmax} at the two sites.

6.2. Results from C0019

Lin et al. (2013) analyzed LWD data collected by JFAST at Site C0019 (Fig. 4b) and integrated these data with compressive strength and core-based observations to determine the stress state and to infer stress history at this site. Although borehole breakouts are present throughout the hanging wall of the plate boundary, they show a wide range in orientations at shallow structural levels (<500 mbsf), suggesting that S_{Hmax} and S_{hmin} are close in magnitude, and/or that S_{Hmax} orientation is highly variable with depth. At deeper levels (>500 mbsf) S_{Hmax} shows a clear trend to the northwest ($319 \pm 23°$), which is sub-parallel to the plate convergence vector of 292° at this location (Fig.4b; Argus et al., 2011). Lin et al. (2013) also used the width of the borehole breakouts and the results of initial shipboard experiments on the unconfined compressive strength (UCS) of sediments from two depth intervals to determine the stress magnitudes. Their results show that the frontal part of the prism above the plate boundary fault is in, or close to, a normal faulting regime (Fig. 6c). These results contrast with core-scale observations, however, that show dominantly thrusting and horizontal shortening with only limited evidence of extension at relatively shallow structural levels. Based on these results, the authors suggested a distinct coseismic stress change from a reverse faulting stress regime before the earthquake to a normal faulting stress regime after the earthquake (Fig. 7). This interpretation is well-consistent with Hasegawa et al. (2012).

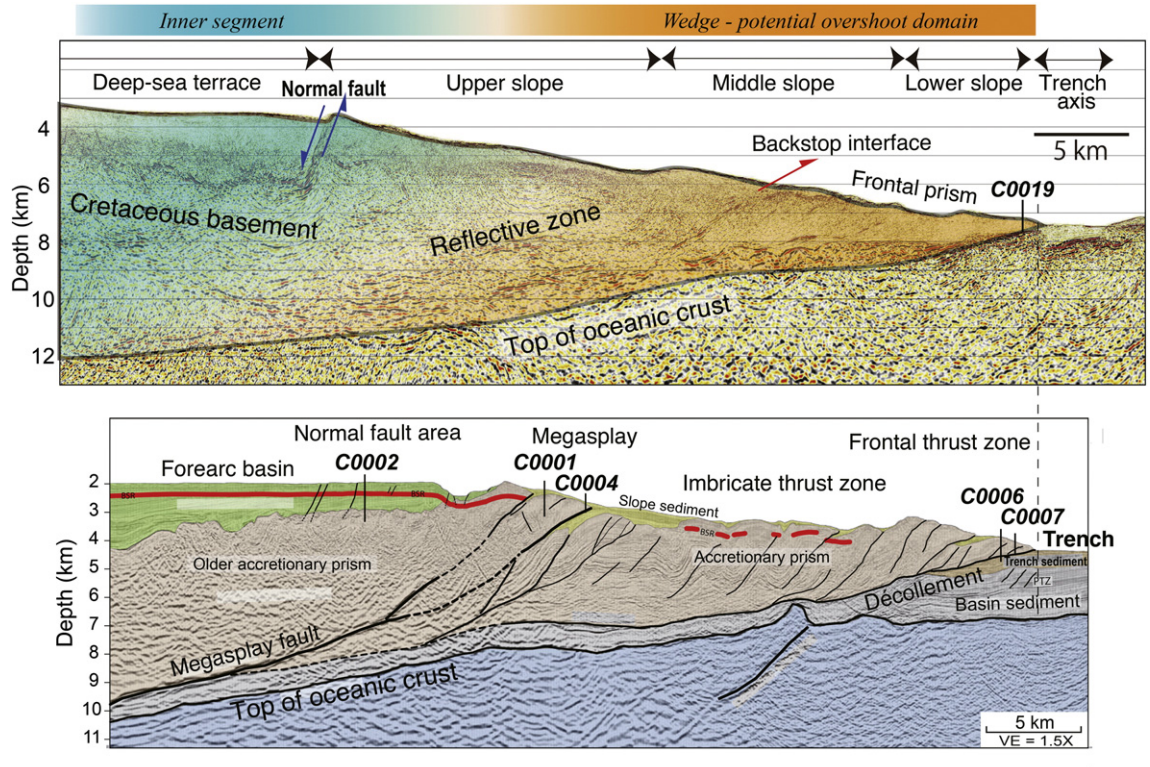

Fig. 5. A comparison of seismic reflection profiles of NanTroSEIZE transect and around JFAST drilling site in the same scale (modified from Moore et al., 2009 and Kodaira et al., 2012 respectively) shows the overall similar structures. The five structure horizontal areas, the deep sea terrace, the upper, middle and lower slopes and the trench axis were defined by Kodaira et al. (2012). Site C0006 in the Nankai subduction zone is at the similar location as Site C0019 in the Japan Trench. At exact location of C0019 no wider seismic profile is available, thus we used this profile locating just 15 km north of C0019.

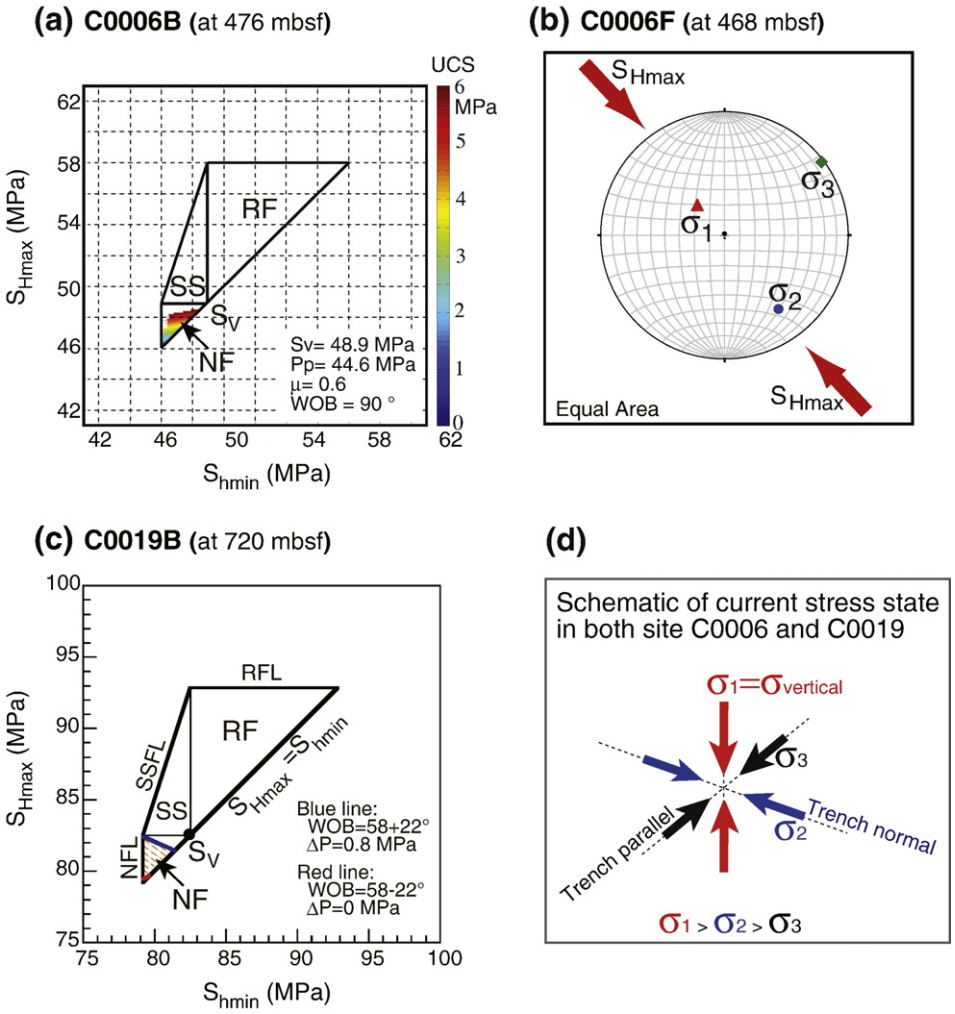

Fig. 6. A comparison of stress states in the hanging wall of the frontal plate-interfaces in toe of Nankai and Japan Trench subduction zones revealed from Sites C0006 and C0019. (a) Possible stress state at 476 mbsf in borehole C0006B constrained from breakout width and assumed wall rock unconfined compressive strength (UCS) locates in the area of normal faulting stress regime (Wu et al., 2013). (b) Stress state at 468 mbsf in borehole C0006F determined from ASR measurements is of normal faulting stress regime being consistent with that from breakouts in C0006B (Byrne et al., 2009). (c) Possible stress state at 720 mbsf in borehole C0019B constrained from breakout width and measured UCS 3.8 MPa locates in the area of normal faulting stress regime (Lin et al., 2013). (d) Schematic of the current common stress state in the hanging wall of the frontal plate-interfaces in both Sites C0006 and C0019.

6.3. Results from ODP Sites 1150 and 1151

FMS and caliper data from Sites 1150 and 1151 were used to define the orientation of S_{Hmax} at these two sites, which were drilled prior to the Tohoku-Oki earthquake. The FMS images showed the development of drilling induced tensile fractures (DITF) and borehole breakouts at deeper structural levels (e.g., >700 mbsf) and the caliper data provide a general constraint on the orientation of borehole breakouts. Although there is variability between the two sites, the combined data set shows S_{Hmax} trending northwest, generally parallel to the plate convergence vector (Lin et al., 2011) (Fig. 4b). Based on the presence of DITFs at both sites and significant seismic activity associated with northwest–southeast directed shortening, Lin et al. (2011) concluded that the hanging of the plate boundary in this area possibly was in a thrusting regime before the 2011 earthquake.

7. Comparison between Nankai and Japan Trench

The general comparison of the Nankai and Tohoku margins presented above shows that the margins share important similarities as well as at least one critical difference (Fig. 5). First, available data suggest that both margins are dominated by an extensional stress regime with a vertically oriented maximum principal stress. Extension along the Tohoku area is show by the dominance of normal faulting aftershocks in the hanging wall above the décollement (Tsuji et al., 2013) as well as the in situ stress data from Site C0019. Extension along Nankai is documented by seismic reflection data along the shelf edge and observations from 3 drill sites that span the accretionary prism. Horizontal compression may occur at deeper levels and in the hanging wall of the megasplay, but normal faulting appears to be the dominant pattern. The second similarity is that both margins can be divided into inner and outer wedges separated by a regionally significant normal fault or a complex system of normal and oblique slip faults. At Tohoku, a landward dipping normal fault with significant offset separates a deep-sea terrace from the upper, middle and low slope that define the accretionary wedge. At Nankai, the seaward edge of the forearc basin is marked by relatively intricate set of normal faults associated with a graben-like structure that marks shelf edge. Some of the normal faults may also have oblique slip that accommodate strike-parallel motion related to moderately oblique plate convergence (Martin et al., 2010). Finally, one critical difference appears to be the presence of a megasplay in the accretionary prism of the Nankai margin and the apparent absence of similar structures along the Tohoku margin.

Interestingly, the similarities of the two margins are also the primary characteristics of margins that typically produce tsunami earthquakes

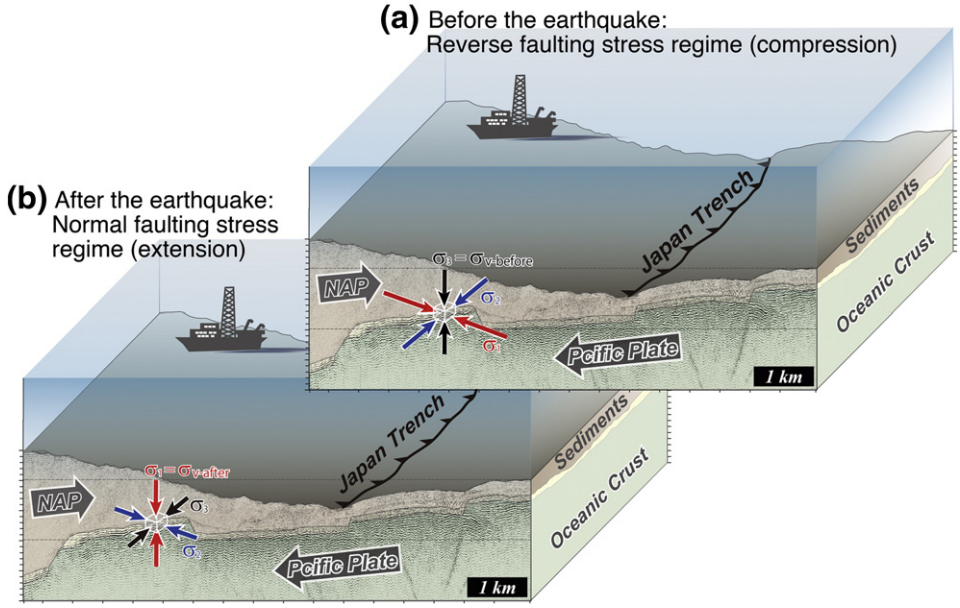

Fig. 7. Schematic of inferred coseismic three-dimensional stress state change from a reverse faulting regime before the Tohoku-oki earthquake (a) to a normal faulting regime after the earthquake (b) in the lower portion of the frontal prism in Japan Trench subduction zone obtained from JFAST (modified from Lin et al., 2013). NAP denotes North American Plate. Red arrows indicate the maximum principal stress (σ_1); blue arrows: the intermediate principal stress (σ_2); black arrows: the minimum principal stress (σ_3). Because the static vertical stress (σ_v) is under a mechanical equilibrium state with the overburden pressure (the gravity of the formations above the depth), the magnitude of σ_v may not change before and after the earthquake; however was the σ_3 before the earthquake, the σ_1 after the earthquake according to the changes of horizontal stress magnitudes during the earthquake.

(McKenzie and Jackson, 2012; Tsuji et al., 2013). For example, recent theoretical studies (McKenzie and Jackson, 2012) as well as recent observations from Tohoku (Tsuji et al., 2013) suggest that tsunamigenic earthquakes result from the simultaneous slip along the décollement and a landward-dipping normal fault or a suite of normal faults that separate the inner and outer wedges. McKenzie and Jackson (2012) also propose that displacements on these regional-scale faults and the seaward motion of the outer wedge are driven by the release of gravitational potential energy as well as elastic strain. Although McKenzie and Jackson (2012) do not address what processes cause the décollement and the normal fault to fail simultaneously, Kimura et al. (2012) suggest that progressive dewatering of underthrust sediments along the Tohoku margin lead to failure and "runaway" slip along the décollement probably weakened by over pore pressure (e.g. Hashimoto et al., 2013; Kitajima and Saffer, 2012; Tobin and Saffer, 2009; Tsuji et al., 2014). Tsuji et al. (2013), based on sea floor observations of extension cracks and heat flow anomalies, also propose that normal faulting in the hanging wall occurred simultaneously with slip on the décollement. Along the Nankai margin, the décollement is also interpreted to be anomalously weak and the seaward edge of the Kumano Basin is deformed exclusively by normal faults, suggesting a tectonic setting similar to Tohoku. One possibility, therefore, is that during a historic great earthquake, which also produced a tsunami along southwest Japan, slip occurred simultaneously on normal faults in the hanging wall and along the décollement.

A complication to this interpretation is that models of the 1944 tsunami suggest that a significant amount of the coseismic slip occurred on the megasplay rather than the décollement (Cummins et al., 2001; Tanioka and Satake, 2001). However, Sakaguchi et al. (2011a), based on observations from Site C0007 which is near the toe of the prism, show that the décollement also moved co-seismically, although the timing of co-seismic slip is unknown. If the model proposed for Tohoku (McKenzie and Jackson, 2012) also applies to the 1944 event along the Kumano transect, then movement along both the megasplay and the décollement must have driven forward motion of the accretionary wedge.

We therefore propose that the two margins represent similar states between tsunami earthquakes, although there are differences. Following this interpretation, the stress state of the accretionary wedge, including the frontal plate interface builds up from a normal faulting stress regime just after a large earthquake to a reverse faulting regime before the next earthquake. In other words, the tectonic horizontal stress caused by plate convergence gradually builds up during the interseismic period and dynamically drops during an earthquake consistent with the conventional stress accumulation fundamental model (e.g. see Kanamori and Brodsky, 2001). Following this interpretation, both Sites C0006 (Nankai) and Site C0019 (Tohoku) appear to be in the early stages of the interseismic cycle with σ_1 is vertical and that S_{Hmax} (interpreted to be σ_2) is generally parallel to the plate convergence vector (Fig. 6). In Nankai margin, more than 60 years have passed from the previous M8-class earthquake propagated through the megasplay fault to the time of drilling at C0006 (2007), but the time length from the previous great earthquake occurred on the décollement and propagated to C0006 is unknown. Hypothetically, the stress state may indicate that in Nankai margin, it is still in an early stage of the interseismic cycle of a great earthquake which occurs on the décollement and propagates to the toe, even cuts the seafloor.

Acknowledgments

This research used data provided by the IODP. The authors gratefully acknowledge helpful discussions with NanTroSEIZE scientists and JFAST scientists and the support provided by EPMs, logging staffs, and laboratory technicians of the expeditions. We really thank the two reviewers, Serge Lallemand and Yoshitaka Hashimoto, for their careful reading and constructive comments which helped us to improve this manuscript. We also appreciate assistance by Miho Sasaoka (SASAMI Geo-Science Inc.) for creating Figure 7. Part of these works were supported by Grants-in-Aid for Scientific Research 25287134 (JSPS), and 21107006 (MEXT), Japan.

References

Ando, M., 1975. Source mechanisms and tectonic significance of historical earthquakes along the Nankai Trough, Japan. Tectonophysics 27, 119–140.

Apel, E.V., Burgmann, R., Steblov, G., Vasilenko, N., King, R., Prytkov, A., Apel, E.V., Burgmann, R., Steblov, G., Vasilenko, N., King, R., Prytkov, A., 2006. Independent active microplate tectonics of northeast Asia from GPS velocities and block modeling. Geophys. Res. Lett. 33, L11303. http://dx.doi.org/10.1029/2006GL026077.

Argus, D.F., Gordon, R.G., DeMets, C., 2011. Geologically current motion of 56 plates relative to the no-net-rotation reference frame. Geochem. Geophys. Geosyst. 12, Q11001. http://dx.doi.org/10.1029/2011GC003751.

Bangs, N., Moore, G.F., Gulick, S.P.S., Pangborn, E.M., Tobin, H.J., Kuramoto, S., Taira, A., 2009. Broad, weak regions of the Nankai Megathrust and implications for shallow coseismic slip. Earth Planet. Sci. Lett. 284, 44–49.

Byrne, T., Fisher, D., 1990. Evidence for a weak and overpressured décollement beneath sediment-dominated accretionary prisms. J. Geophys. Res. 95, 9081–9097.

Byrne, T., Lin, W., Tsutsumi, A., Yamamoto, Y., Lewis, J., Kanagawa, K., Kitamura, Y., Yamaguchi, A., Kimura, G., 2009. Anelastic strain recovery reveals extension across SW Japan subduction zone. Geophys. Res. Lett. 36, L01305. http://dx.doi.org/10.1029/2009GL040749.

Chang, C., McNeill, L.C., Moore, J.C., Lin, W., Conin, M., Yamada, Y., 2010. In situ stress state in the Nankai accretionary wedge estimated from borehole wall failures. Geochem. Geophys. Geosyst. 11, Q0AD04. http://dx.doi.org/10.1029/2010GC003261.

Chester, F.M., Mori, J.J., Toczko, S., Eguchi, N., The Expedition 343/343T Scientists, 2012. Japan Trench Fast Drilling Project (JFAST). IODP Prel. Rept. 343/343T. http://dx.doi.org/10.2204/iodp.pr.343343T.2012.

Conin, M., Henry, P., Bourlange, S., Raimbourg, H., Reuschle, T., 2011. Interpretation of porosity and LWD resistivity from the Nankai accretionary wedge in the light of clay physicochemical properties: evidence for erosion and local overpressuring. Geochem. Geophys. Geosyst. 12, Q0AD07.

Conin, M., Henry, P., Godard, V., Bourlange, S., 2012. 2012. Splay fault slip in a subduction margin, a new model of evolution. Earth Planet. Sci. Lett. 341, 170–175.

Conin, M., Bourlange, S., Henry, P., Boiselet, A., Gaillot, P., 2014. Distribution of resistive and conductive structures in Nankai accretionary wedge reveals contrasting stress paths. Tectonophysics 611, 181–191.

Cummins, P.R., Hori, T., Kaneda, Y., 2001. Splay fault and megathrust earthquake slip in the Nankai Trough. Earth Planets Space 53, 235–241.

Expedition 314 Scientists, 2009a. Expedition 314 Site C0001. In: Kinoshita, M., Tobin, H., Ashi, J., Kimura, G., Lallement, S., Screaton, E.J., Curewitz, D., Masago, H., Moe, K.T., the Expedition 314/315/316 Scientists (Eds.), Proc. IODP 314/315/316. Integrated Ocean Drilling Program Management International, Inc., Washington, DC. http://dx.doi.org/10.2204/iodp.proc.314315316.113.2009.

Expedition 314 Scientists, 2009b. Expedition 314 Site C0004. In: Kinoshita, M., Tobin, H., Ashi, J., Kimura, G., Lallement, S., Screaton, E.J., Curewitz, D., Masago, H., Moe, K.T., the Expedition 314/315/316 Scientists (Eds.), Proc. IODP 314/315/316. Integrated Ocean Drilling Program Management International, Inc., Washington, DC. http://dx.doi.org/10.2204/iodp.proc.314315316.116.2009.

Expedition 314 Scientists, 2009c. Expedition 314 Site C0006. In: Kinoshita, M., Tobin, H., Ashi, J., Kimura, G., Lallemant, S., Screaton, E.J., Curewitz, D., Masago, H., Moe, K.T., the Expedition 314/315/316 Scientists (Eds.), Proc. IODP 314/315/316. Integrated Ocean Drilling Program Management International, Inc, Washington, DC. http://dx.doi.org/10.2204/iodp.proc.314315316.118.2009.

Expedition 315 Scientists, 2009. Expedition 315 Site C0002. In: Kinoshita, M., Tobin, H., Ashi, J., Kimura, G., Lallemant, S., Screaton, E.J., Curewitz, D., Masago, H., Moe, K.T., the Expedition 314/315/316 Scientists (Eds.), Proc. IODP 314/315/316. Integrated Ocean Drilling Program Management International, Inc., Washington, DC. http://dx.doi.org/10.2204/iodp.proc.314315316.124.2009.

Expedition 319 Scientists, 2010. Site C0010. In: Saffer, D., McNeill, L., Byrne, T., Araki, E., Toczko, S., Eguchi, N., Takahashi, K., The Expedition 319 Scientists (Eds.), Proc. IODP 319. Integrated Ocean Drilling Program Management International, Inc., Tokyo. http://dx.doi.org/10.2204/iodp.proc.319.104.2010.

Expedition 322 Scientists, 2010. Site C0011. In: Saito, S., Underwood, M.B., Kubo, Y., The Expedition 322 Scientists (Eds.), Proc. IODP 322. Integrated Ocean Drilling Program Management International, Inc, Tokyo. http://dx.doi.org/10.2204/iodp.proc.322.103.2010.

Gulick, S.P., Bangs, N., Moore, G., Ashi, J., Martin, K.M., Sawyer, D., Tobin, H., Kuramoto, S., Taira, A., 2010. Rapid forearc basin uplift and megasplay fault development from 3D seismic images of Nankai margin off Kii Peninsula, Japan. Earth Planet. Sci. Lett. 300, 55–62. http://dx.doi.org/10.1016/j.epsl.2010.09.034.

Haimson, B.C., Cornet, F.H., 2003. ISRM suggested methods for rock stress estimation—part 3: hydraulic fracturing (HF) and/or hydraulic testing of pre-existing fractures (HTPF). Int. J. Rock Mech. Min. Sci. 40, 1011–1020.

Haq, S.S.B., Davis, D.M., 2008. Extension during active collision in thin-skinned wedges: insights from laboratory experiments. Geology 36, 475–478.

Hardebeck, J.L., 2004. Stress triggering and earthquake probability estimates. J. Geophys. Res. 109, B04310. http://dx.doi.org/10.1029/2003JB002437.

Hasegawa, A., Yoshida, K., Asano, Y., Okada, T., Iinuma, T., Ito, Y., 2012. Change in stress field after the 2011 great Tohoku–Oki earthquake. Earth Planet. Sci. Lett. 355–356, 231–243. http://dx.doi.org/10.1016/j.epsl.2012.08.042.

Hashimoto, Y., Doi, N., Tsuji, T., 2013. Difference in acoustic properties at seismogenic fault along a subduction interface: application to estimation of effective pressure and fluid pressure ratio. Tectonophysics 600, 134–141. http://dx.doi.org/10.1016/j.tecto.2013.03.016.

Hashimoto, Y., Eida, M., Ueda, Y., 2014. Changes in paleostress state along a subduction zone preserved in an on-land accretionary complex, the Yokonami mélange in the Cretaceous Shimanto Belt, Kochi, southwest Japan. Tectonics 33, 2045–2058. http://dx.doi.org/10.1002/2013TC003487.

Heki, K., Miyazaki, S., 2001. Plate convergence and long-term crustal deformation in Central Japan. Geophys. Res. Lett. 28, 2313–2316.

Hirose, T., Saffer, D.M., Tobin, H.J., Toczko, S., Maeda, L., Kubo, Y., Kimura, G., Moore, G.F., Underwood, M.B., Kanagawa, K., 2013. NanTroSEIZE Stage 3: NanTroSEIZE plate boundary deep riser 3. IODP Sci. Prosp. 348. http://dx.doi.org/10.2204/iodp.sp.348.2013

Hsu, Y.-J., Yu, S.-B., Simons, M., Kuo, L.-C., Chen, H.-Y., 2009. Interseismic crustal deformation in the Taiwan plate boundary zone revealed by GPS observations, seismicity, and earthquake focal mechanisms. Tectonophysics. http://dx.doi.org/10.1016/j.tecto.2008.11.016.

Ide, S., Baltay, A., Beroza, G.C., 2011. Shallow dynamic overshoot and energetic deep rupture in the 2011 *Mw* 9.0 Tohoku-Oki earthquake. Science 332, 1426–1429. http://dx.doi.org/10.1126/science.1207020.

Ienaga, M., McNeill, L.C., Mikada, H., Saito, S., Goldberg, D., Moore, J.C., 2006. Borehole image analysis of the Nankai Accretionary Wedge, ODP Leg 196: Structural and stress studies. Tectonophysics 426, 207–220. http://dx.doi.org/10.1016/j.tecto.2006.02.018.

Ito, T., Funato, A., Lin, W., Doan, M.-L., Boutt, D.F., Kano, Y., Ito, H., Saffer, D., McNeill, L.C., Byrne, T., Moe, K.T., 2013. Determination of stress state in deep subsea formation by combination of hydraulic fracturing in situ test and core analysis: a case study in the IODP Expedition 319. J. Geophys. Res. Solid Earth 118. http://dx.doi.org/10.1002/jgrb.50086.

Kamei, R., Pratt, R.G., Tsuji, T., 2012. Waveform tomography imaging of a megasplay fault system in the seismogenic Nankai subduction zone. Earth Planet. Sci. Lett. 317–318, 343–353.

Kanamori, H., 1972. Tectonic implications of the 1944 Tonankai and the 1946 Nankaido earthquakes. Phys. Earth Planet. Inter. 5, 129–139.

Kanamori, H., Brodsky, E., 2001. The physics of earthquakes. Phys. Today 54 (6), 34. http://dx.doi.org/10.1063/1.1387590.

Kimura, G., Moore, G., Strasser, M., Screaton, E., Curewitz, D., Streiff, C., Tobin, H., 2011. Spatial and temporal evolution of the megasplay fault in the Nankai Trough. Geochem. Geophys. Geosyst. 12, Q0A008. http://dx.doi.org/10.1029/2010GC003335.

Kimura, G., et al., 2012. Runaway slip to the trench due to rupture of highly pressurized megathrust beneath the middle trench slope: the tsunamigenesis of the 2011 Tohoku earthquake off the east coast of northern Japan. Earth Planet. Sci. Lett. 339–340, 32–45. http://dx.doi.org/10.1016/j.epsl.2012.08.042.

Kinoshita, M., Tobin, H., 2013. Interseismic stress accumulation at the locked zone of Nankai Trough seismogenic fault off Kii Peninsula. Tectonophysics 600, 153–164. http://dx.doi.org/10.1016/j.tecto.2013.03.015.

Kinoshita, M., Tobin, H., Moe, K.T., The Expedition 314 Scientists, 2008. NanTroSEIZE Stage 1A: NanTroSEIZE LWD Transect. IODP Prel. Rept. 314. http://dx.doi.org/10.2204/iodp.pr.314.2008

Kitajima, H., Saffer, D.M., 2012. Elevated pore pressure and anomalously low stress in regions of low frequency earthquakes along the Nankai Trough subduction megathrust. Geophys. Res. Lett. 39, L23301. http://dx.doi.org/10.1029/2012GL053793.

Kitamura, Y., Kanamatsu, T., Zhao, X., 2010. Structural evolution in accretionary prism toe revealed by magnetic fabric analysis from IODP NanTroSEIZE Expedition 316. Earth Planet. Sci. Lett. 292, 221–230.

Kodaira, S., et al., 2012. Coseismic fault rupture at the trench axis during the 2011 Tohoku-oki earthquake. Nat. Geosci. 5, 646–650. http://dx.doi.org/10.1038/NGEO1547.

Lallemand, S., Funiciello, F., 2009. Subduction Zone Geodynamics. Springer, Berlin.

Lallemant, S.J., Byrne, T., Maltman, A., Karig, D., Henry, P., 1993. Stress tensors at the toe of the Nankai accretionary prism: an application of inverse methods to slickenlined faults. Proceedings of the Ocean Drilling Program, Scientific Results 131, pp. 103–122.

Lee, H., Chang, C., Ong, S.H., Song, I., 2013. Effect of anisotropic borehole wall failures when estimating in situ stresses: a case study in the Nankai accretionary wedge. Mar. Pet. Geol. 48, 411–422. http://dx.doi.org/10.1016/j.marpetgeo.2013.09.004.

Lewis, J., Byrne, T., Kanagawa, K., 2013. Evidence for mechanical decoupling of the upper plate at the Nankai subduction zone: constraints from core-scale faults at NantroSEIZE Sites C0001 and C0002. Geochem. Geophys. Geosyst. 14, 620–633. http://dx.doi.org/10.1029/2012GC004406.

Lin, W., et al., 2007. Current stress state and principal stress rotations in the vicinity of the Chelungpu Fault induced by the 1999 Chi-Chi, Taiwan, earthquake. Geophys. Res. Lett. 34, L16307. http://dx.doi.org/10.1029/2007GL030515.

Lin, W., Yamamoto, K., Ito, H., Masago, H., Kawamura, Y., 2008. Estimation of minimum principal horizontal stress from an extended leak-off test onboard the Chikyu drilling vessel and suggestions for future test procedures. Sci. Drill. 6, 43–47. http://dx.doi.org/10.2204/iodp.sd.6.06.2008.

Lin, W., et al., 2010a. Present-day principal horizontal stress orientations in the Kumano forearc basin of the southwest Japan subduction zone determined from IODP NanTroSEIZE drilling Site C0009. Geophys. Res. Lett. 37, L13303. http://dx.doi.org/10.1029/2010GL043158.

Lin, W., Byrne, T., Yamamoto, Yuhji, Yamamoto, Yuzuru, 2010b. Preliminary results of three-dimensional stress orientation in the accretionary prism in Nankai Subduction Zone. Japan by anelastic strain recovery measurements of core samples retrieved from IODP NanTroSEIZE Site C0009. Abstract T13A-2151 presented at 2010 Fall Meeting. AGU, San Francisco, CA, USA.

Lin, W., Saito, S., Sanada, Y., Yamamoto, Y., Hashimoto, Y., Kanamatsu, T., 2011. Principal horizontal stress orientations prior to the 2011 M_w 9.0 Tohoku-Oki, Japan, earthquake in its source area. Geophys. Res. Lett. 38, L00G10. http://dx.doi.org/10.1029/2011GL049097.

Lin, W., Conin, M., Moore, J.C., Chester, F.M., Nakamura, Y., Mori, J.J., Anderson, L., Brodsky, E.E., Eguchi, H., Expedition 343 Scientists, 2013. Stress state in the largest displacement area of the 2011 Tohoku-Oki earthquake. Science 339, 687–690. http://dx.doi.org/10.1126/science. 1229379.

Loveless, J.P., Meade, B.J., 2010. Geodetic imaging of plate motions, slip rates, and partitioning of deformation in Japan. J. Geophys. Res. 115, B02410. http://dx.doi.org/10.1029/2008JB006248.

Ma, K.-F., Chan, C.-H., Stein, R.S., 2005. Response of seismicity to Coulomb stress triggers and shadows of the 1999 Mw = 7.6 Chi-Chi, Taiwan, earthquake. J. Geophys. Res. 110, B05S19. http://dx.doi.org/10.1029/2004JB003389.

Martin, K.M., Gulick, S.P.S., Bangs, N.L.B., Moore, G.F., Ashi, J., Park, J.-O., Kuramoto, S., Taira, A., 2010. Possible strain partitioning structure between the Kumano fore-arc basin

and the slope of the Nankai Trough accretionary prism. Geochem. Geophys. Geosyst. 11, Q0AD02. http://dx.doi.org/10.1029/2009GC002668.
McKenzie, D., Jackson, J., 2012. Tsunami earthquake generation by the release of gravitational potential energy. Earth Planet. Sci. Lett. 345–348, 1–8.
McNeill, L.C., et al., 2004. Deformation and in situ stress in the Nankai Accretionary Prism from resistivity-at-bit images, ODP Leg 196. Geophys. Res. Lett. 31, L02602. http://dx.doi.org/10.1029/2003GL018799.
McNeill, L.C., Saffer, D.M., Byrne, T., Araki, E., Toczko, S., Eguchi, N., Takahashi, K., Expediion 319 Scientists, 2010. IODP Expedition 319, NanTroSEIZE stage 2: first IODP riser drilling operations and observatory installation towards understanding subduction zone seismogenesis. Sci. Drill. 10, 4–13. http://dx.doi.org/10.2204/iodp.sd.10.01.2010.
Miyazaki, S., Heki, K., 2001. Crustal velocity field of southwest Japan: subduction and arc–arc collision. J. Geophys. Res. 106 (B3), 4305–4326. http://dx.doi.org/10.1029/2000JB900312.
Moore, G.F., Park, J.-O., Bangs, N.L., Gulick, S.P., Tobin, H.J., Nakamura, Y., Sato, S., Tsuji, T., Yoro, T., Tanaka, H., Uraki, S., Kido, Y., Sanada, Y., Kuramoto, S., Taira, A., 2009. Structural and seismic stratigraphic framework of the NanTroSEIZE Stage 1 transect. In: Kinoshita, M., Tobin, H., Ashi, J., Kimura, G., Lallement, S., Screaton, E.J., Curewitz, D., Masago, H., Moe, K.T., The Expedition 314/315/316 Scientists (Eds.), Proc. IODP 314/315/316. Integrated Ocean Drilling Program Management International, Inc, Washington, DC. http://dx.doi.org/10.2204/iodp.proc.314315316.102.2009.
Moore, J.C., Chang, C., Mcneill, L.C., Moe, T.K., Yamada, Y., Huftile, G., 2011. Growth of borehole breakouts with time after drilling: implications for state of stress, NanTroSEIZE transect, SW Japan. Geochem. Geophys. Geosyst. 12, Q04D09. http://dx.doi.org/10.1029/2010GC003417.
Moore, G.F., Boston, B.B., Sacks, A.F., Saffer, D.M., 2013. Analysis of normal fault populations in the Kumano Forearc Basin, Nankai Trough, Japan: 1 multiple orientations and generations of faults from 3-D coherency mapping. Geochem. Geophys. Geosyst. 114, 1989–2002. http://dx.doi.org/10.1002/ggge.20119.
Mori, J.J., Chester, F.M., Eguchi, N., Toczko, S., 2012. Japan Trench Fast Earthquake Drilling Project (JFAST). IODP Sci. Prosp. 343. http://dx.doi.org/10.2204/iodp.sp.343.2012
Olcott, K., Saffer, D., 2012. Constraints on in situ stress across the shallow megasplay fault offshore the Kii Peninsula. SW Japan from borehole breakouts. Abstract T13A-2576 presented at 2012 Fall Meeting. AGU, San Francisco, Calif, pp. 3–7 (Dec.).
Ozawa, S., Nishimura, T., Suito, H., Kobayashi, T., Tobita, M., Imakiire, T., 2011. Coseismic and postseismic slip of the 2011 magnitude-9 Tohoku-Oki earthquake. Nature 475, 373–376. http://dx.doi.org/10.1038/nature10227.
Park, J.-O., Fujie, G., Wijerathne, L., Hori, T., Kodaira, S., Fukao, Y., Moore, G.F., Bangs, N.L., Kuramoto, S., Taira, A., 2010. A low-velocity zone with weak reflectivity along the Nankai subduction zone. Geology 38, 283–286. http://dx.doi.org/10.1130/G30205.1.
Sacks, A., Saffer, D.M., Fisher, D., 2013. Analysis of normal fault populations in the Kumano forearc basin, Nankai Trough, Japan: 2. Principal axes of stress and strain from inversion of fault orientations. Geochem. Geophys. Geosyst. 14, 1973–1988.
Saffer, D.M., et al., 2009. NanTroSEIZE stage 2: NanTroSEIZE riser/riserless observatory. IODP Prel. Rept. 319. http://dx.doi.org/10.2204/iodp.pr.319.2009
Saffer, D.M., Flemings, P.B., Boutt, D., Doan, M.-L., Ito, T., McNeill, L., Byrne, T., Conin, M., Lin, W., Kano, Y., Araki, E., Eguchi, N., Toczko, S., 2013. In situ stress and pore pressure in the Kumano Forearc Basin, offshore SW Honshu from downhole measurements during riser drilling. Geochem. Geophys. Geosyst. 14, 1454–1470. http://dx.doi.org/10.1002/ggge.20051.
Saito, S., Underwood, M.B., Kubo, Y., 2009. NanTroSEIZE stage 2: subduction inputs. IODP Sci. Prosp. 322. http://dx.doi.org/10.2204/iodp.sp.322.2009
Sakaguchi, A., Chester, F., Curewitz, D., Fabbri, O., Goldsby, D., Kimura, G., Li, C.-F, Masaki, Y., Screaton, E.J., Tsutsumi, A., Ujiie, K., Yamaguchi, A., 2011a. Seismic slip propagation to the updip end of plate boundary subduction interface faults: vitrinite reflectance geothermometry on Integrated Ocean Drilling Program NanTroSEIZE cores. Geology 39, 395–398. http://dx.doi.org/10.1130/G31642.1.
Sakaguchi, A., Kimura, G., Strasser, M., Screaton, E.J., Curewitz, D., Murayama, M., 2011b. Episodic seafloor mud brecciation due to great subduction zone earthquakes. Geology 39, 919–922. http://dx.doi.org/10.1130/G32043.1.
Seeber, L., Armbruster, J.G., 2000. Earthquakes as beacons of stress change. Nature 407, 69–72.
Sella, G.F., Dixon, T.H., Mao, A., 2002. REVEL: a model for recent plate velocities from space geodesy. J. Geophys. Res. 107 (B4), 2081. http://dx.doi.org/10.1029/2000JB000033.
Simons, M., Minson, S.E., Sladen, A., Ortega, F., Jiang, J., Owen, S.E., Meng, L., Ampuero, J.-P., Wei, S., Chu, R., Helmberger, D.V., Kanamori, H., Hetland, E., Moore, A.W., Webb, F.H., 2011. The 2011 magnitude 9.0 Tohoku-Oki earthquake: mosaicking the megathrust from seconds to centuries. Science 332, 1421–1425. http://dx.doi.org/10.1126/science.1206731.
Song, I., Saffer, D.M., Flemings, P.B., 2011. Mechanical characterization of slope sediments: constraints on in situ stress and pore pressure near the tip of the megasplay fault in the Nankai accretionary complex. Geochem. Geophys. Geosyst. 12, Q0AD17. http://dx.doi.org/10.1029/2011GC003556.
Stein, R.S., 1999. The role of stress transfer in earthquake occurrence. Nature 402, 605–609.
Strasser, M., Moore, G.F., Kimura, G., Kopf, A.J., Underwood, M.B., Guo, J., Screaton, E.J., 2011. Slumping and mass transport deposition in the Nankai fore arc: evidence from IODP drilling and 3-D reflection seismic data. Geochem. Geophys. Geosyst. 12, Q0AD13. http://dx.doi.org/10.1029/2010GC003431.
Tanioka, Y., Satake, K., 2001. Coseismic slip distribution of the 1946 Nankai earthquake and aseismic slips caused by the earthquake. Earth Planets Space 53, 235–241.
Tobin, H.J., Kinoshita, M., 2006. Investigations of seismogenesis at the Nankai Trough, Japan. IODP Sci. Prosp. NanTroSEIZE Stage 1. http://dx.doi.org/10.2204/iodp.sp.nantroseize1.2006.
Tobin, H.J., Saffer, D.M., 2009. Elevated fluid pressure and extreme mechanical weakness of a plate boundary thrust, Nankai Trough subduction zone. Geology 37, 679–682. http://dx.doi.org/10.1130/G25752A.1.
Tobin, H., Kinoshita, M., Ashi, J., Lallemant, S., Kimura, G., Screaton, E., Moe, K.T., Masago, H., Curewitz, D., The Expedition 314/315/316 Scientists, 2009a. NanTroSEIZE Stage 1 expeditions: introduction and synthesis of key results. In: Kinoshita, M., Tobin, H., Ashi, J., Kimura, G., Lallement, S., Screaton, E.J., Curewitz, D., Masago, H., Moe, K.T., The Expedition 314/315/316 Scientists (Eds.), Proc. IODP 314/315/316, 10.2204/iodp.proc.314315316.101.2009 Integrated Ocean Drilling Program Management International, Inc., Washington, DC.
Tobin, H., Kinoshita, M., Moe, K.T., The Expedition 314 Scientists, 2009b. Expedition 314 Summary, in *NanTroSEIZE* Stage 1: Investigations of Seismogenesis. Nankai Trough, Japan, Proc. ICD *314/315/316*, 10.2204/iodp.proc. 314315316.111.2009.
Tsuji, T., Dvorkin, J., Mavko, G., Nakata, N., Matsuoka, T., Nakanishi, A., Kodaira, S., Nishizawa, O., 2011a. Vp/Vs ratio and shear-wave splitting in the Nankai Trough seismogenic zone: insights into effective stress, pore pressure and sediment consolidation. Geophysics 76, WA71–WA82.
Tsuji, T., et al., 2011b. In situ stress state from walkaround VSP anisotropy in the Kumano basin southeast of the Kii Peninsula, Japan. Geochem. Geophys. Geosyst. 12, Q0AD19. http://dx.doi.org/10.1029/2011GC003583.
Tsuji, T., Kawamura, K., Kanamatsu, T., Kasaya, T., Fujikura, K., Ito, Y., Tsuru, T., Kinoshita, M., 2013. Extension of continental crust by anelastic deformation during the 2011 Tohoku-oki earthquake: the role of extensional faulting in the generation of a great tsunami. Earth Planet. Sci. Lett. 364, 44–58. http://dx.doi.org/10.1016/j.epsl.2012.12.038.
Tsuji, T., Kamei, R., Pratt, R.G., 2014. Porepressure distribution of a mega-splay fault system in the Nankai Trough subduction zone: insight into up-dip extent of the seismogenic zone. Earth Planet. Sci. Lett. 364, 44–58. http://dx.doi.org/10.1016/j.epsl.2012.12.038.
Wang, K., Hu, Y., 2006. J. Geophys. Res. 111, B06410. http://dx.doi.org/10.1029/2005JB004094.
Wu, H.-Y., Kinoshita, M., Sanada, Y., 2012. Stress state estimation by geophysical logs in NanTroSEIZE Expedition 319-Site C0009, Kumano Basin, southwest Japan. Geophys. Res. Lett. 39, L18303. http://dx.doi.org/10.1029/2012GL053086.
Wu, H.-Y., Chan, C.-H., Kinoshita, M., Saito, S., 2013. Stress field observation and modeling from the NanTroSEIZE scientific drillings in the Nankai Trough system, SW Japan. Tectonophysics 600, 99–107. http://dx.doi.org/10.1016/j.tecto.2013.04.009.
Yamada, Y., Shibanuma, J., 2015. Small-scale stress fluctuations in borehole breakouts and their implication in identifying potential active faults around the seismogenic megasplay fault, Nankai Trough, SW Japan. Earth Planets Space 67, 17. http://dx.doi.org/10.1186/s40623-014-0176-9.
Yamamoto, Yuzuru, Lin, W., Oda, H., Byrne, T., Yamamoto, Yuhji, 2013. Stress states at the subduction input site, Nankai Subduction Zone, using anelastic strain recovery (ASR) data in the basement basalt and overlying sediments. Tectonophysics 600, 91–98. http://dx.doi.org/10.1016/j.tecto.2013.01.028.